A GENERAL SOLUTION FOR ACTIVE AND PASSIVE PRESSURES ON A VERTICAL PLANE IN A SLOPING EARTH MASS OF INFINITE LENGTH

by

GLEN LEROY MARTIN

A THESIS

submitted to

OREGON STATE COLLEGE

in partial fulfillment of
the requirements for the
degree of

MASTER OF SCIENCE

June 1961

APPROVED:

Signature redacted for privacy.

Professor of Civil Engineering

In Charge of Major

Signature redacted for privacy.

Head of Department of Civil Engineering

Signature redacted for privacy.

Chairman of School Graduate Committee

Signature redacted for privacy.

Dean of Graduate School

Date thesis is presented APRIL 18, 1961

Typed by Glen L. Martin

ACKNOWLEDGEMENTS

The writer wishes to acknowledge helpful suggestions from Professors Martin P. Coopey and Glenn W. Holcomb in the preparation of this thesis. Dr. Charles Behlke's assistance in reviewing foreign literature and suggestions on the preparation of the charts were very helpful as were the suggestions of Dr. Harry Goheen of the Department of Mathematics in the analytical development. To all of these gentlemen the writer expresses his appreciation.

Although the writer's wife, Theolyn, has not contributed in a technical nature, this paper would not have been completed without her continued encouragement and self sacrifice - to her a special note of thanks.

TABLE OF CONTENTS

A GENERAL SOLUTION FOR ACTIVE AND PASSIVE PRESSURES ON A VERTICAL PLANE IN A SLOPING EARTH MASS OF INFINITE LENGTH

INTRODUCTION

The first of two classical earth pressure theories was advanced by Coulomb's sliding wedge analysis in 1773. In 1860 Rankine presented his theory of lateral earth pressures which is based on conjugate stress relationships between the vertical stress and the lateral pressure on a vertical plane.

Rankine's original development considered a dry cohesionless material with either a horizontal or a sloping surface. Rankine's work was analytical and was later adapted to Mohr's stress circle for graphical solution.

Bell, in 1915, extended Rankine's work to include dry cohesive soils by a graphic method of solution (1, p. 124-150). This graphical solution made use of Mohr's stress circle but in an inconvenient manner.

This paper presents the analytical solution for lateral pressures based on the Rankine assumptions. The solution is general in that it includes cohesionless and cohesive soils as well as horizontal or sloping surfaces. The limitations imposed on the solution are that no seepage pressures are acting in the slope and the plane of investigation is vertical.

The graphical procedures which are being used for the determination of lateral pressures are time consuming and therefore to some extent are not desireable. The solution of the equation developed in this paper would also be time consuming, however, charts are enclosed which greatly simplify the operation.

REVIEW OF STRESSES ON A VERTICAL PLANE IN AN INFINITE SLOPE

The Rankine state of stress assumes that at failure the soil is in a state of plastic equilibrium and the soil will be deformed in a direction parallel to the surface such that two limiting stress conditions on a vertical plane exist.

The first of these states comes into being when the element ABCD in Figure 1(a) tends to deform by elongation parallel to the surface as shown in Figure 1(b) and is known as the active state of stress. The other state of stress is approached as the soil tends to deform by shortening parallel to the surface as shown in Figure 1(c) and is known as the passive state of stress. With the vertical stress on a plane parallel to the surface remaining constant, the active state of stress is the minimum stress that will maintain equilibrium while the passive state of stress is the maximum stress that will maintain equilibrium.

The element ABCD is chosen such that AB and CD are parallel to EF, and AC and BD are vertical. The selection of the unit distance parallel to the surface is convenient since the surface of the selected element will then have a unit area when considering a unit thickness normal to the plane ABCD. The vertical stress, S, acting on AB is then equal to the weight above the element.

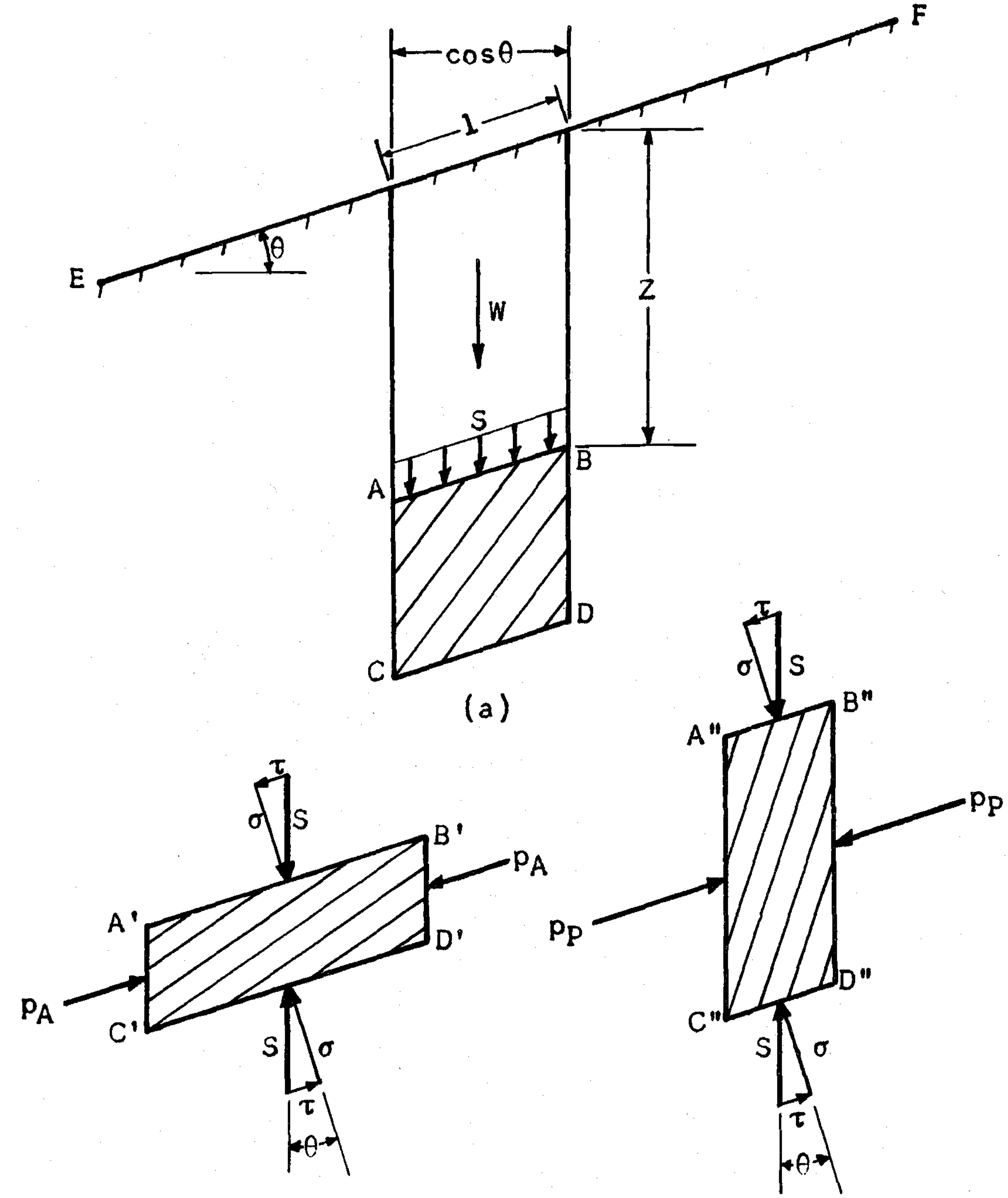

FIGURE 1

The horizontal distance across the parallelopiped thus formed will be equal to the $\cos\theta$ as shown, and the volume of the parallelopiped is $Z\cos\theta$. The weight, W, as well as the vertical stress on AB, will then be $\gamma Z\cos\theta$, where γ is the unit weight of the soil.

This vertical stress, S, is the vector sum of the two components shown in either Figure 1(b) or 1(c). The component normal to the surface of the element, σ_{AB}, is equal to $S\cos\theta$ while the tangential stress, τ_{AB}, is equal to $S\sin\theta$. Since $S=W=\gamma Z\cos\theta$ it follows that $\sigma_{AB}=\gamma Z\cos^2\theta$ and $\tau_{AB}=\gamma Z\cos\theta\sin\theta$.

ADAPTATION TO MOHR'S CIRCLE OF STRESSES

When these stresses are plotted on Mohr's coordinates, Figure 2(a), it can be seen that the vector sum, S, of the two components σ_{AB} and τ_{AB} may be used directly when measured along a line oriented identically to the slope.

The sign convention for Mohr's coordinates used in this paper will be consistent with that used in soil mechanics where normal compressive stresses are positive and counterclockwise shear stresses are positive.

Incorporating Mohr's rupture envelope with Figure 2(a) yields the basic structure of Figure 2(b), where the angle of friction, φ, and the unit cohesion, c, are the strength characteristics of the soil.

The leaves of this envelope, UV and U'V', delineate stress conditions of failure from those of stability. All stress conditions representing failure would fall in the crosshatched zone. When the normal and shear stresses on a plane through an elemental volume are such that they fall on the lines UV or U'V' the elemental volume of material is in a state of plastic equilibrium and failure of the material is imminent.

The stress conditions on all of the planes through the elemental volume, normal to the plane ABCD, are expressed by Mohr's circle of stresses.

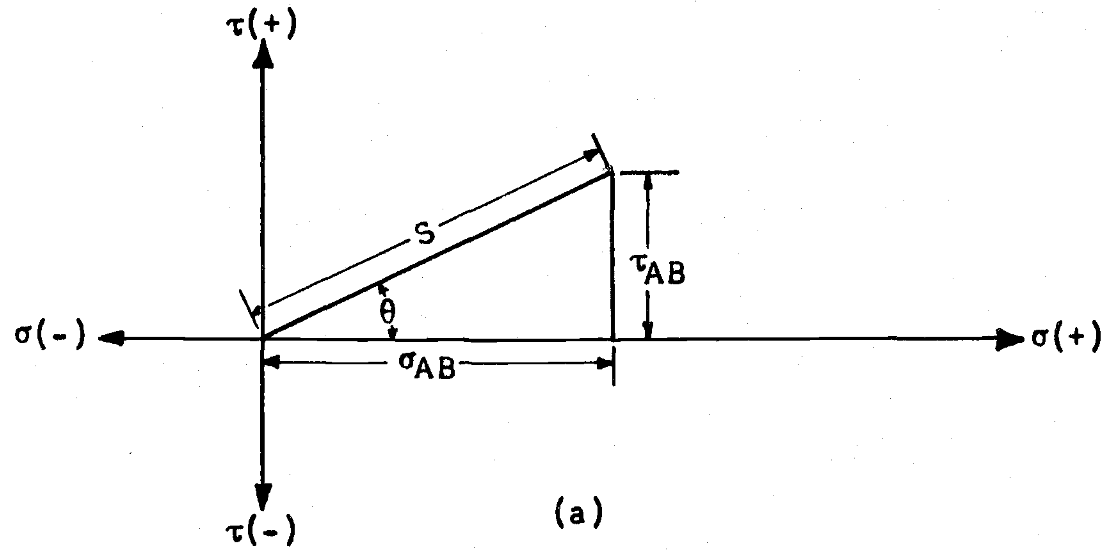
τ(+)
S
τ_{AB}
θ
σ(-)
σ(+)
σ_{AB}
τ(-)

(a)

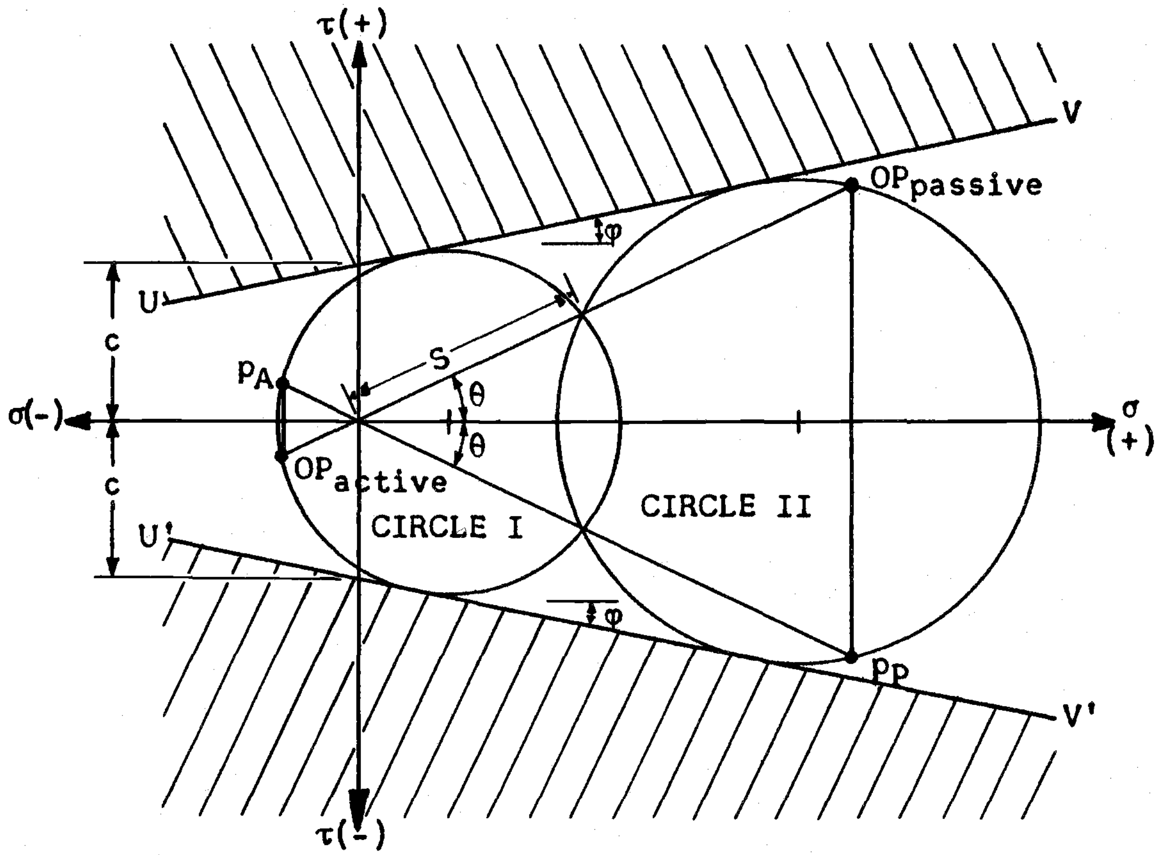
τ(+)
V
$OP_{passive}$
φ
U'
c
S
p_A
θ
σ(-)
σ
(+)
θ
OP_{active}
c
CIRCLE I
CIRCLE II
U'
φ
p_P
V'
τ(-)

(b)

FIGURE 2

In the cases under consideration the stresses on the plane parallel to the surface are known. If failure is impending, the stress condition on one of the planes through the element must be coincident with one of the leaves of Mohr's rupture envelope. These two conditions may be met, as well as the condition that the center of the circle of stresses lies on the line of zero shear stress, by the two circles of stress shown in Figure 2(b).

Circle I represents the stresses in the element at the active case of failure, while circle II represents the stresses in the element during the passive case of failure.

Mohr's circle of stresses, since its original presentation in 1882, has been modified in many ways to expedite its use. The use of this circle in this paper, with the single angle and origin of planes modifications, may be outlined by the following steps:

(1) Through the point of known stress condition on Mohr's circle of stresses draw a line parallel to the plane on which these stresses act.

(2) The point where this line again intersects the circle of stresses is the origin of all of the planes normal to plane ABCD in the element, and is known as the origin of planes or OP.

(3) To find the stress condition on any other plane through the elemental volume, construct a line

through the origin of planes parallel to the plane on which the stresses are desired.

(4) The point at which the line thus constructed again intersects the circle of stresses is the stress condition on the desired plane.

Applying these steps to circle I, Figure 2(b), the active stress, p_A, on a vertical plane in the elemental volume ABCD of Figure 1(a) may be determined as shown in Figure 2(b).

By symmetry about the line designating zero shear stress it is seen that the point representing the active stress on the vertical plane lies at the intersection of the circle of stresses and a line drawn through the origin of coordinates, inclined at an angle θ from the line of zero shear stress. The distance from the origin of coordinates to this intersection is identical to the distance between the origin of coordinates and the origin of planes, OP. A similar situation exists for the passive pressures, p_P, on a vertical plane as shown in Figure 2(b).

Thus the magnitudes of the active and passive pressures on a vertical plane may be found by determining the distance from the origin of coordinates to the respective origin of planes.

THE ANALYTICAL DEVELOPMENT

The solution of the problem is accomplished by solving the unknown stress conditions (σ_A, τ_A, σ_P, and τ_P) in terms of the known stress conditions (σ_1 and τ_1), the strength characteristics of the soil (φ and c), and the angle of the slope measured from the horizontal (θ). The interrelationships are shown graphically in Figure 3.

It will suffice to use the terms σ_2 and τ_2 in place of σ_A, τ_A, σ_P, and τ_P since a single derivation yields a quadratic equation giving both solutions.

The equation of the leaf of Mohr's rupture envelope shown in Figure 3 is:

$$\tau-\sigma\tan\varphi-c = 0 \qquad (1)$$

Since the radius of Mohr's circle of stress must be normal to this leaf we may write the equation:

$$-\frac{\sigma\tan\varphi}{\sqrt{1+\tan^2\varphi}}+\frac{\tau}{\sqrt{1+\tan^2\varphi}}-\frac{c}{\sqrt{1+\tan^2\varphi}} = 0 \qquad (2)$$

which is the normal form of Equation (1) and is the equation of all lines normal to the line given by Equation (1).

To find the length of the line between the rupture envelope and the point (σ_0,τ_0) which is perpendicular to the rupture envelope, coordinates of the point ($\sigma=\sigma_0$ and $\tau=\tau_0=0$) are substituted in Equation (2) which gives (4, p. 63):

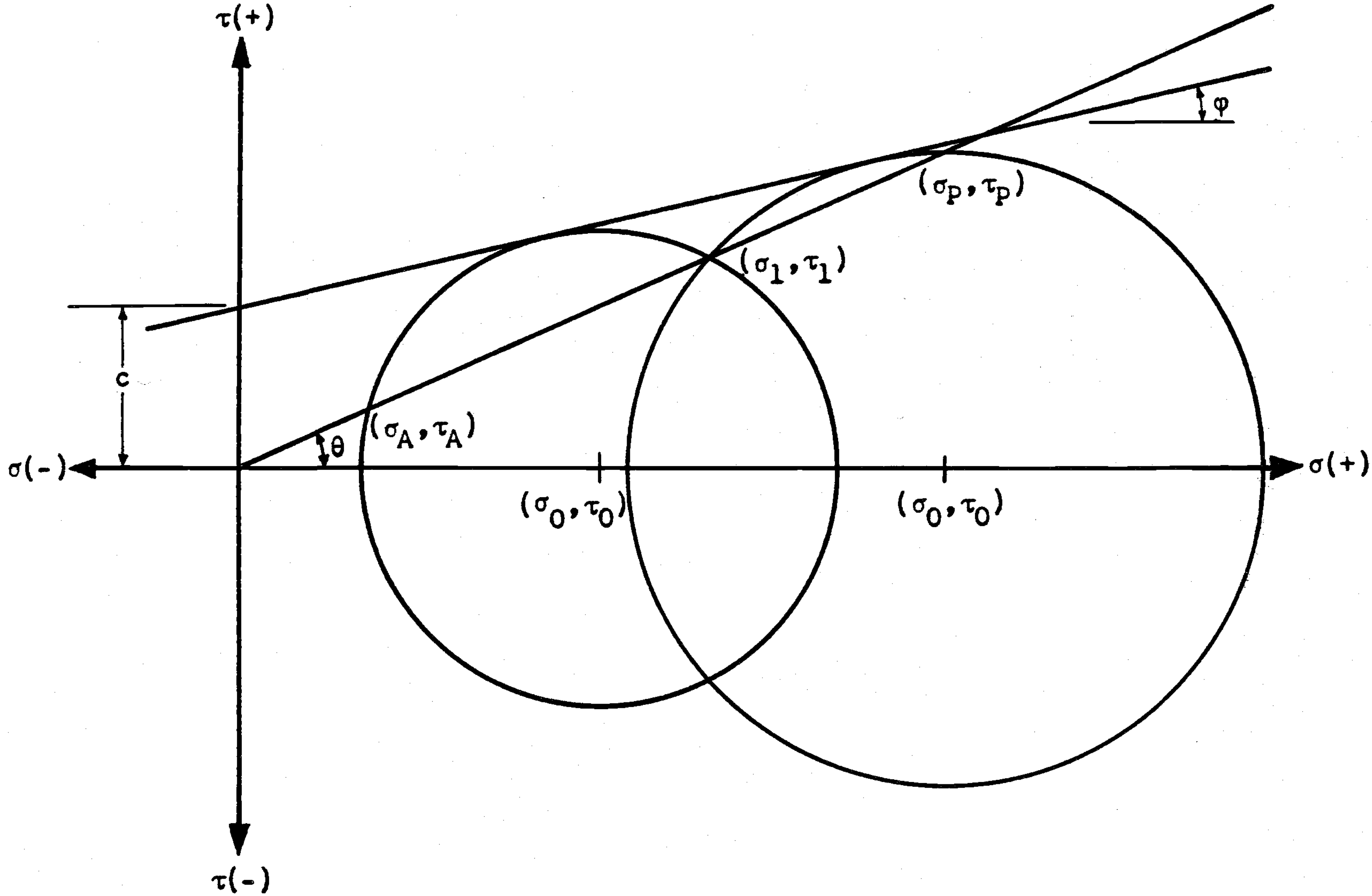

τ(+)
φ
(σ_p, τ_p)
(σ_1, τ_1)
c
(σ_A, τ_A)
θ
σ(-)
σ(+)
(σ_0, τ_0)
(σ_0, τ_0)
τ(-)

FIGURE 3

$$r = \left| -\frac{\sigma_0 \tan\varphi}{\sqrt{1+\tan^2\varphi}} - \frac{c}{\sqrt{1+\tan^2\varphi}} \right| \tag{3}$$

which is the radius of Mohr's circle of stresses.

The equation of the stress circle is then:

$$(\sigma-\sigma_0)^2 + \tau^2 - \frac{(\sigma_0 \tan\varphi+c)^2}{(1+\tan^2\varphi)} = 0 \tag{4}$$

when $\sigma=\sigma_1$ and $\tau=\tau_1=\sigma_1\tan\theta$ the equation of the stress circle is:

$$(\sigma_1-\sigma_0)^2 + (\sigma_1\tan\theta)^2 - \frac{(\sigma_0 \tan\varphi+c)^2}{(1+\tan^2\varphi)} = 0 \tag{5}$$

Equation (5) may be written in the form:

$$\sigma_1^2 - \frac{2\sigma_0}{(1+\tan^2\theta)}\sigma_1 + \frac{\sigma_0^2(1+\tan^2\varphi)-(\sigma_0\tan\varphi+c)^2}{(1+\tan^2\theta)(1+\tan^2\varphi)} = 0 \tag{6}$$

The sum of the roots of a quadratic equation in σ_1 is equal to the coefficient of σ_1, with its sign changed, divided by the coefficient of σ_1^2 (5, p. 130) or:

$$\sigma_1 + \sigma_2 = \frac{2\sigma_0}{(1+\tan^2\theta)} \tag{7}$$

Equation (5) may also be written in the form:

$$\sigma_0^2 + (-2\sigma_1-2\sigma_1\tan^2\varphi-2c\tan\varphi)\sigma_0 + [\sigma_1^2(1+\tan^2\varphi+\tan^2\theta+\tan^2\varphi\tan^2\theta)-c^2] = 0 \tag{8}$$

Solving for σ_0 in Equation (8) using the quadratic formula:

$$\sigma_0 = \frac{(2\sigma_1+2\sigma_1\tan^2\varphi+2c\tan\varphi)}{2} \pm \sqrt{\frac{(-2\sigma_1-2\sigma_1\tan^2\varphi-2c\tan\varphi)^2}{4} - \frac{4[\sigma_1{}^2(1+\tan^2\varphi+\tan^2\theta+\tan^2\varphi\tan^2\theta)-c^2]}{4}} \qquad (9)$$

Substituting the value of σ_0 from Equation (9) into Equation (7) and solving for σ_2 gives:

$$\sigma_2 = \frac{(2\sigma_1+2\sigma_1\tan^2\varphi+2c\tan\varphi)}{(1+\tan^2\theta)} \pm \sqrt{\frac{(-2\sigma_1-2\sigma_1\tan^2\varphi-2c\tan\varphi)^2}{(1+\tan^2\theta)^2} - \frac{4[\sigma_1{}^2(1+\tan^2\varphi+\tan^2\theta+\tan^2\varphi\tan^2\theta)-c^2]}{(1+\tan^2\theta)^2}} - \sigma_1 \qquad (10)$$

Equation (10) may be reduced to:

$$\sigma_2 = \frac{\sigma_1(1+2\tan^2\varphi-\tan^2\theta) + 2c\tan\varphi}{(1+\tan^2\theta)} \pm 2\sqrt{\frac{(1+\tan^2\varphi)[\sigma_1{}^2(\tan^2\varphi-\tan^2\theta)+2\sigma_1 c\tan\varphi+c^2]}{(1+\tan^2\theta)^2}} \qquad (11)$$

From Figure 2(a) it can be seen that $\sigma_1=\gamma Z\cos^2\theta$, substituting this value in Equation (11):

$$\sigma_2 = \frac{\gamma Z\cos^2\theta(1+2\tan^2\varphi-\tan^2\theta)+2c\tan\varphi}{(1+\tan^2\theta)} \pm$$

$$2\sqrt{\frac{(1+\tan^2\varphi)[\gamma^2Z^2\cos^4\theta(\tan^2\varphi-\tan^2\theta) + 2c\gamma Z\cos^2\theta\tan\varphi+c^2]}{(1+\tan^2\theta)^2}} \qquad (12)$$

Since $(1+\tan^2\theta)^{-1}=\cos^2\theta$ and simplyfing Equation (12):

$$\sigma_2 = \cos^2\theta[2\gamma Z\cos^2\theta(1+\tan^2\varphi)+2c\tan\varphi-\gamma Z] \pm 2\cos^2\theta\sqrt{(1+\tan^2\varphi)[\gamma Z\cos^2\theta\{\gamma Z\cos^2\theta(1+\tan^2\varphi)+2c\tan\varphi-\gamma Z\}+c^2]} \qquad (13)$$

which is the normal stress on a vertical plane. In order to obtain the resultant stress, p, the normal stress, σ_1, is divided by $\cos\theta$:

$$p = \cos\theta[2\gamma Z\cos^2\theta(1+\tan^2\varphi)+2c\tan\varphi-\gamma Z] \pm 2\cos\theta\sqrt{(1+\tan^2\varphi)[\gamma Z\cos^2\theta\{\gamma Z\cos^2\theta(1+\tan^2\varphi)+2c\tan\varphi-\gamma Z\}+c^2]} \qquad (14)$$

which is the general equation for the active and passive pressures on a vertical plane in a sloping earth mass. The smaller magnitude, using the minus sign of the quadratic solution, yields the active stress, p_A, while the larger magnitude, using the plus sign, gives the passive stress, p_P.

Letting: $G = \cos\theta[2\gamma Z\cos^2\theta(1+\tan^2\varphi)+2c\tan\varphi-\gamma Z]$

and $J = 2\cos\theta\sqrt{(1+\tan^2\varphi)[\gamma Z\cos^2\theta\{\gamma Z\cos^2\theta(1+\tan^2\varphi)+2c\tan\varphi-\gamma Z\}+c^2]}$

the general equations for active and passive pressures may be written:

$$p_A = G - J \tag{15}$$

and $$p_P = G + J \tag{16}$$

CHART SOLUTIONS OF THE GENERAL EQUATION

Since a solution of the general equation each time a stress is desired would be a rather arduous task, charts are enclosed which greatly simplify this operation.

If both sides of Equation (14) are divided by the unit cohesion, c, all terms are dimensionless quantities. Two dimensionless parameters containing four of the six variables are useful in the construction of the charts. They are $c/\gamma Z$ which is set equal to N and p/c which is set equal to K. Substituting K and N in Equation (14) gives:

$$K = \cos\theta\left[\frac{2}{N}\cos^2\theta(1+\tan^2\varphi)+2\tan\varphi-\frac{1}{N}\right] \pm 2\cos\theta\sqrt{(1+\tan^2\varphi)\left[\frac{1}{N}\cos^2\theta\left\{\frac{1}{N}\cos^2\theta(1+\tan^2\varphi)+2\tan\varphi-\frac{1}{N}\right\}+1\right]} \qquad (17)$$

Equation (17) was programmed on an IBM 650 computer and sufficient values of K were determined to construct the charts shown in Figures 4 through 21.

Figures 4 through 12 are for K_A, or the active coefficient, and Figures 13 through 21 give values for K_P, the passive coefficient.

The limits of N were arrived at by setting arbitrary limits on the parameters of which N is a function. It was originally assumed that the unit weight could vary from 20 pounds per cubic foot, the submerged condition, to 130 pounds per cubic foot for the dry dense condition; the unit cohesion, c, would vary from zero, cohesionless soils, to 3,000 pounds per square foot; and Z from one foot to fifty feet. The minimum and maximum values of N are then zero and 150 respectively.

It was found from the computed data that the values of K were very insensitive with N values greater than ten, therefore the charts were not produced beyond this value. Since K varied so rapidly, it appeared impractical, due to space limitations, to extend the curves below an N value of one-tenth.

Example Chart Solution:

Given: c=2,500 pounds per square foot, $\varphi=10^\circ$, γ=100 pounds per cubic foot, and $\theta=20^\circ$.

Required: The passive pressure on a vertical plane 10 feet below the surface.

The applicable chart is shown in Figure 15 which is for K_p and $\varphi=10^\circ$.

$N = c/\gamma Z = 2{,}500/(100)(10) = 2.5$

The value of K_p corresponding to $N=2.5$ and $\theta=20^\circ$ is 2.67.

Since $K_p=p_p/c$, then $p_p=cK_p=(2{,}500)(2.67)=6{,}675$ pounds per square foot.

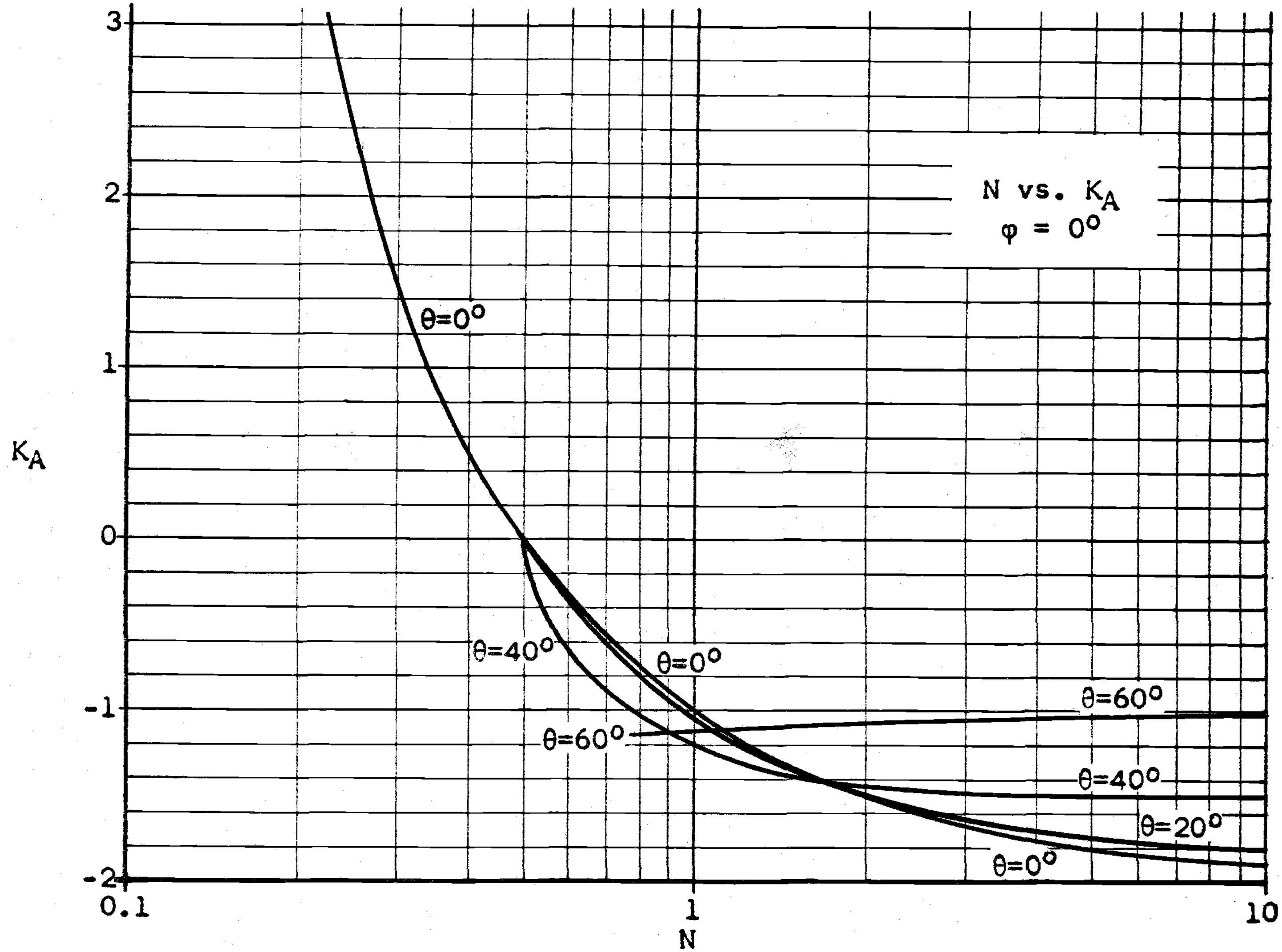

FIGURE 4

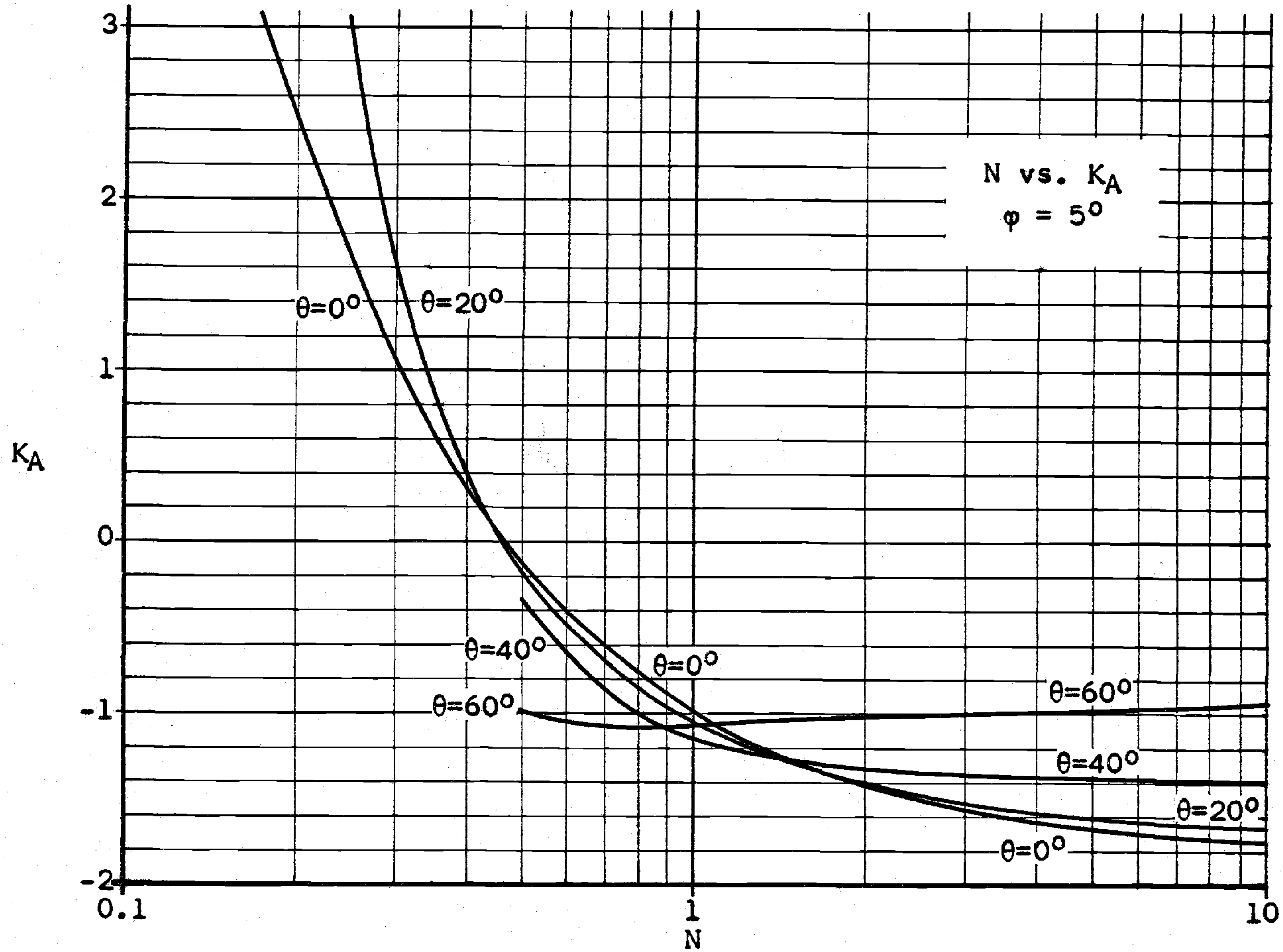
N vs. K_A
$\varphi = 5^\circ$
θ=0°
θ=20°
θ=40°
θ=0°
θ=60°
θ=60°
θ=40°
θ=20°
θ=0°
K_A
3
2
1
0
-1
-2
0.1
1
10
N

FIGURE 5

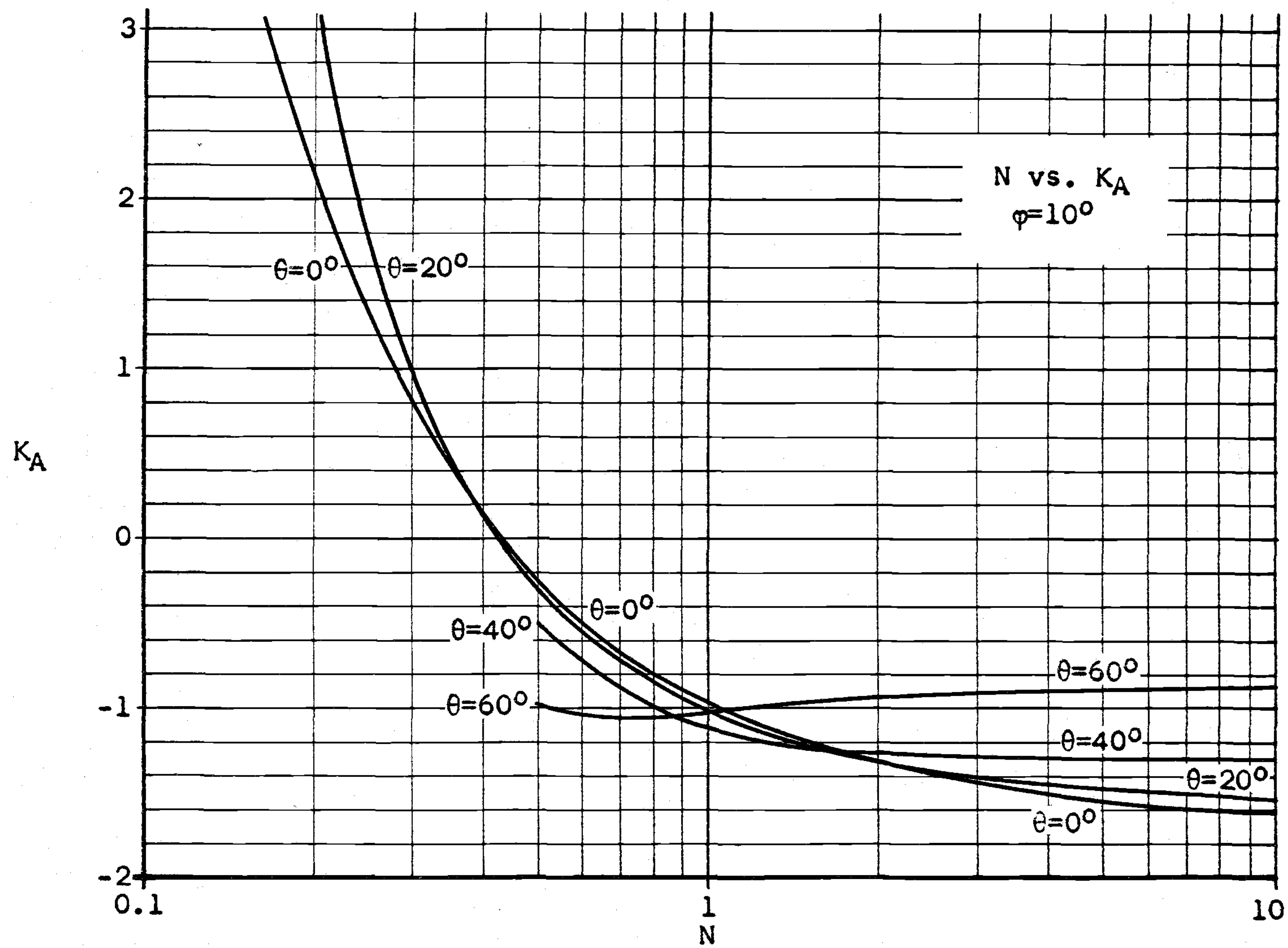
N vs. K_A
φ=10°
K_A
3
2
1
0
-1
-2
0.1
1
10
N
θ=0°
θ=20°
θ=0°
θ=40°
θ=60°
θ=60°
θ=40°
θ=20°
θ=0°

FIGURE 6

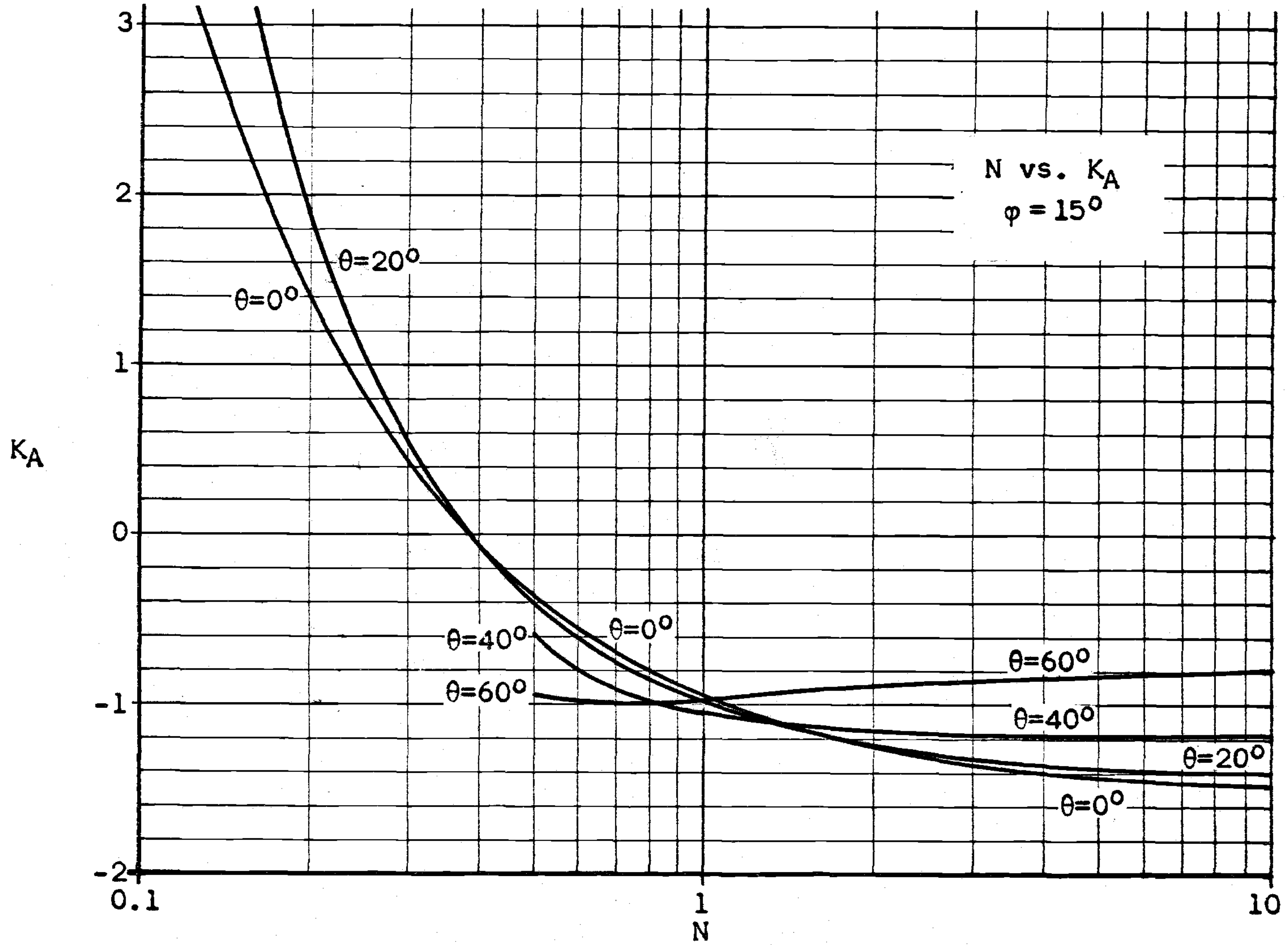
N vs. K_A
$\varphi = 15^\circ$
$\theta=0^\circ$
$\theta=20^\circ$
$\theta=40^\circ$
$\theta=60^\circ$
K_A
N
3
2
1
0
-1
-2
0.1
1
10

FIGURE 7

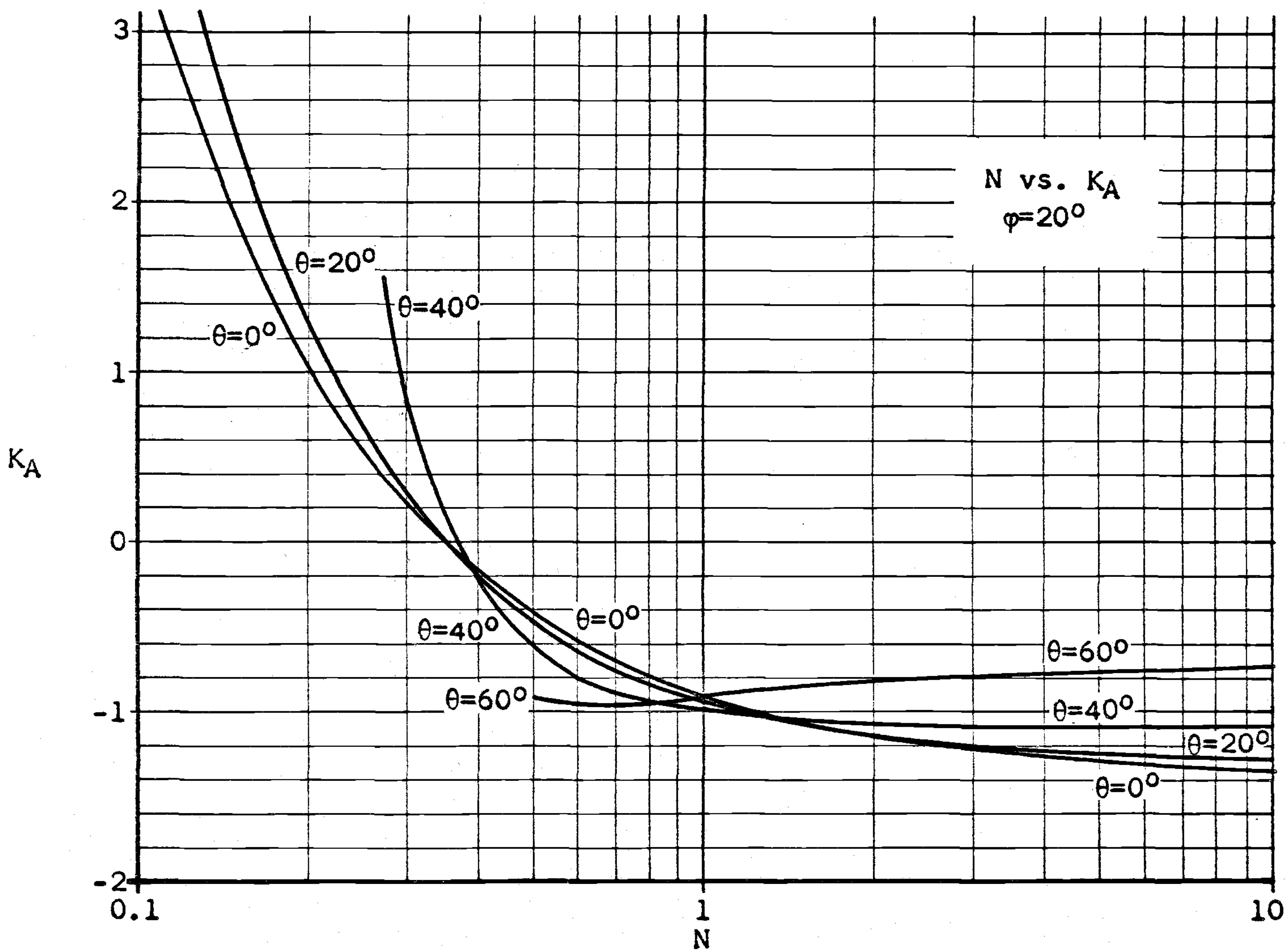
N vs. K_A
φ=20°
θ=20°
θ=40°
θ=0°
θ=40°
θ=0°
θ=60°
θ=60°
θ=40°
θ=20°
θ=0°
K_A
3
2
1
0
-1
-2
0.1
1
10
N

FIGURE 8

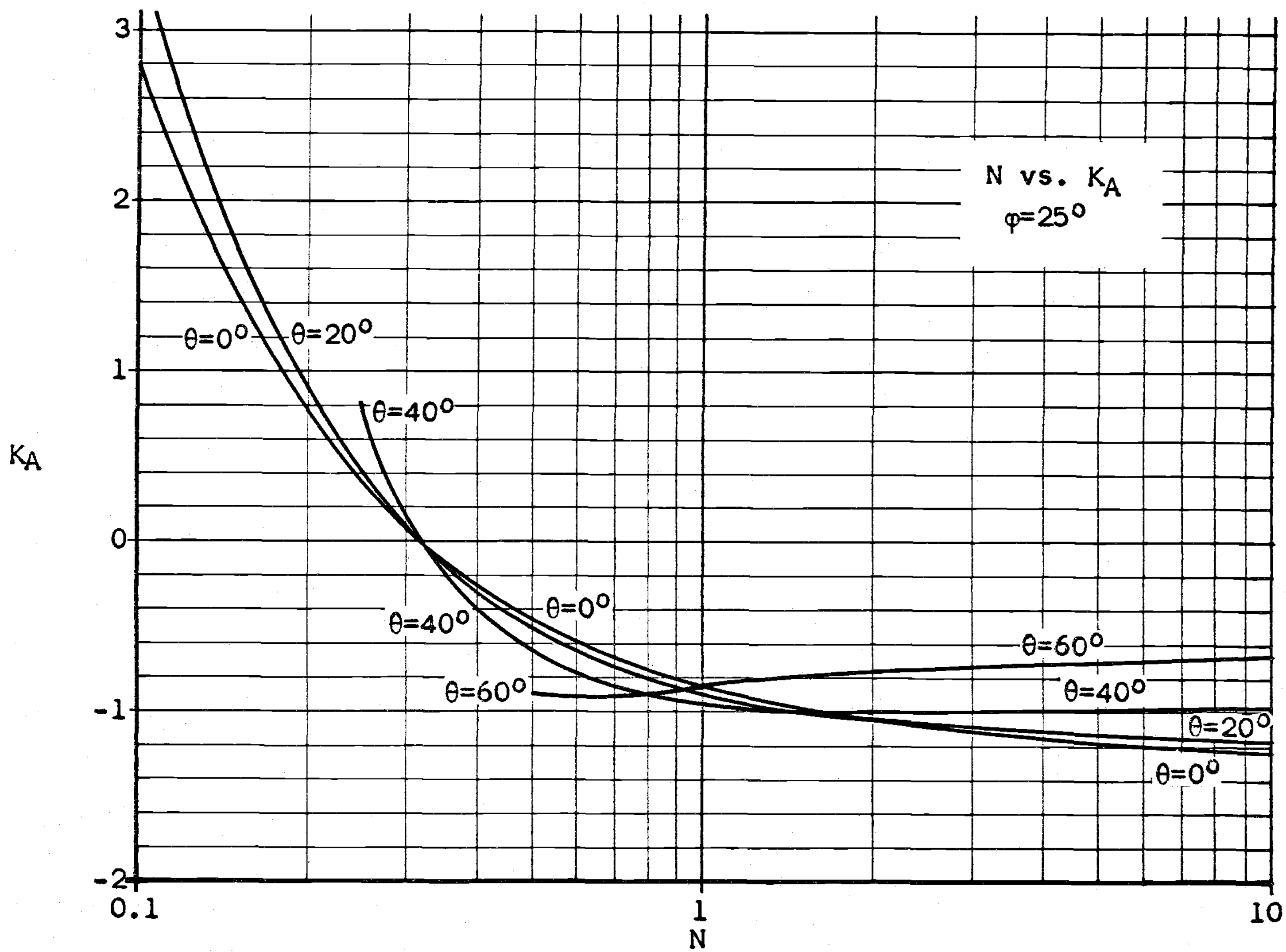
N vs. K_A
$\varphi=25^{\circ}$
$\theta=0^{\circ}$
$\theta=20^{\circ}$
$\theta=40^{\circ}$
$\theta=40^{\circ}$
$\theta=0^{\circ}$
$\theta=60^{\circ}$
$\theta=60^{\circ}$
$\theta=40^{\circ}$
$\theta=20^{\circ}$
$\theta=0^{\circ}$
K_A
3
2
1
0
-1
-2
0.1
1
10
N

FIGURE 9

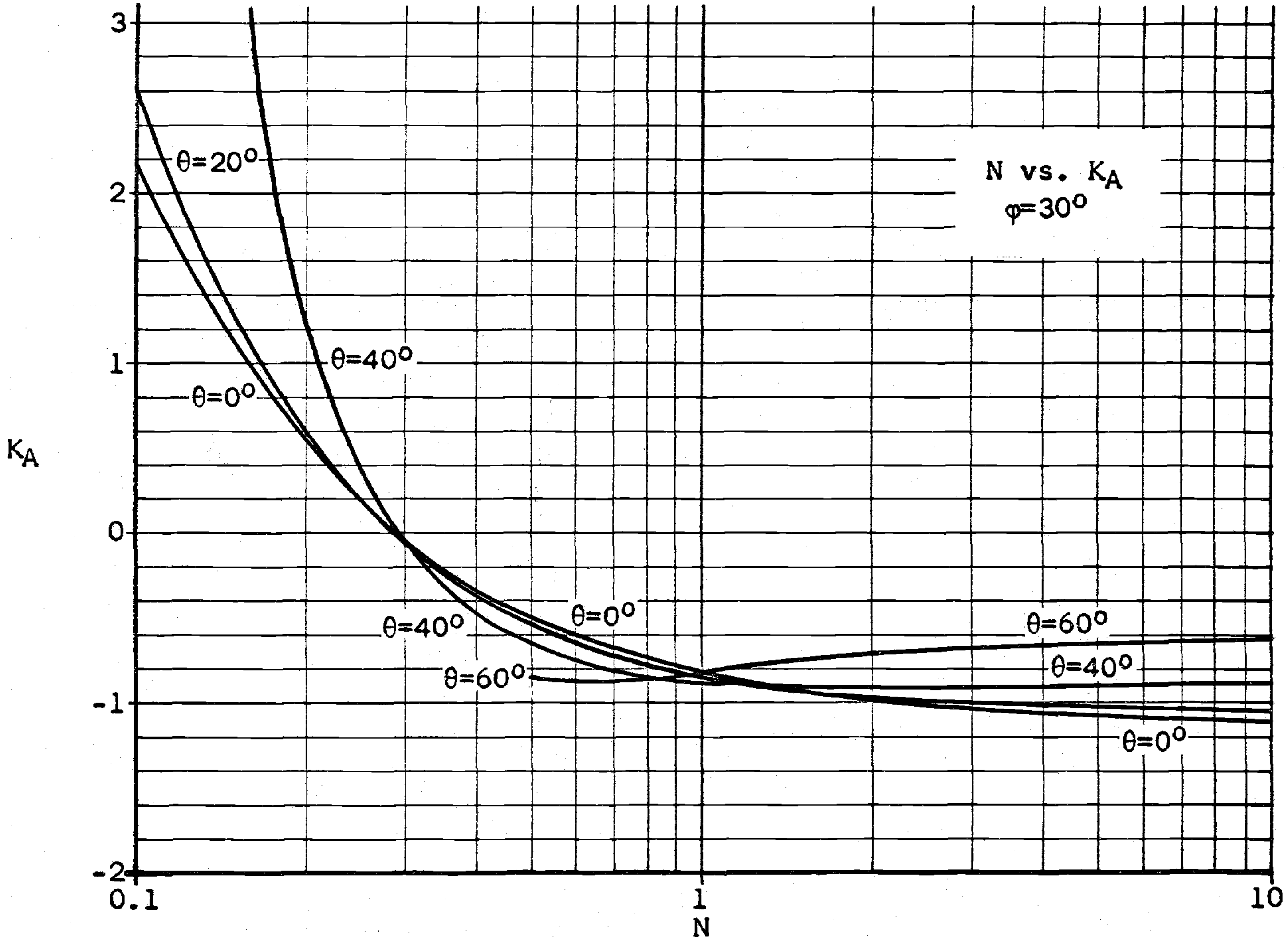
N vs. K_A
$\varphi=30^o$
$\theta=20^o$
$\theta=40^o$
$\theta=0^o$
$\theta=40^o$
$\theta=0^o$
$\theta=60^o$
$\theta=60^o$
$\theta=40^o$
$\theta=0^o$
K_A
N
3
2
1
0
-1
-2
0.1
1
10

FIGURE 10

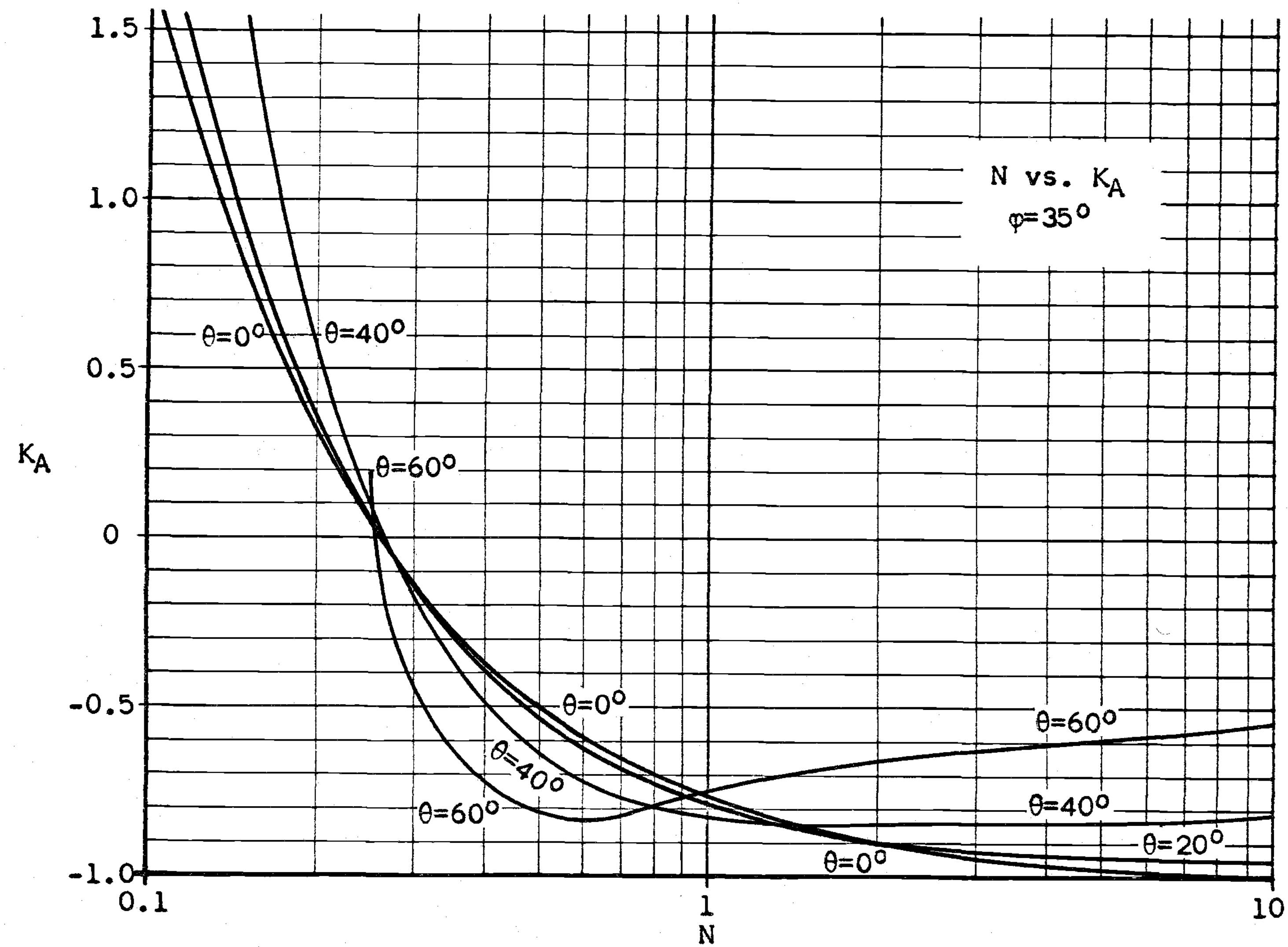

N vs. K_A
φ=35°
1.5
1.0
0.5
0
-0.5
-1.0
0.1
1
10
N
K_A
θ=0°
θ=40°
θ=60°
θ=0°
θ=40°
θ=60°
θ=60°
θ=40°
θ=20°
θ=0°

FIGURE 11

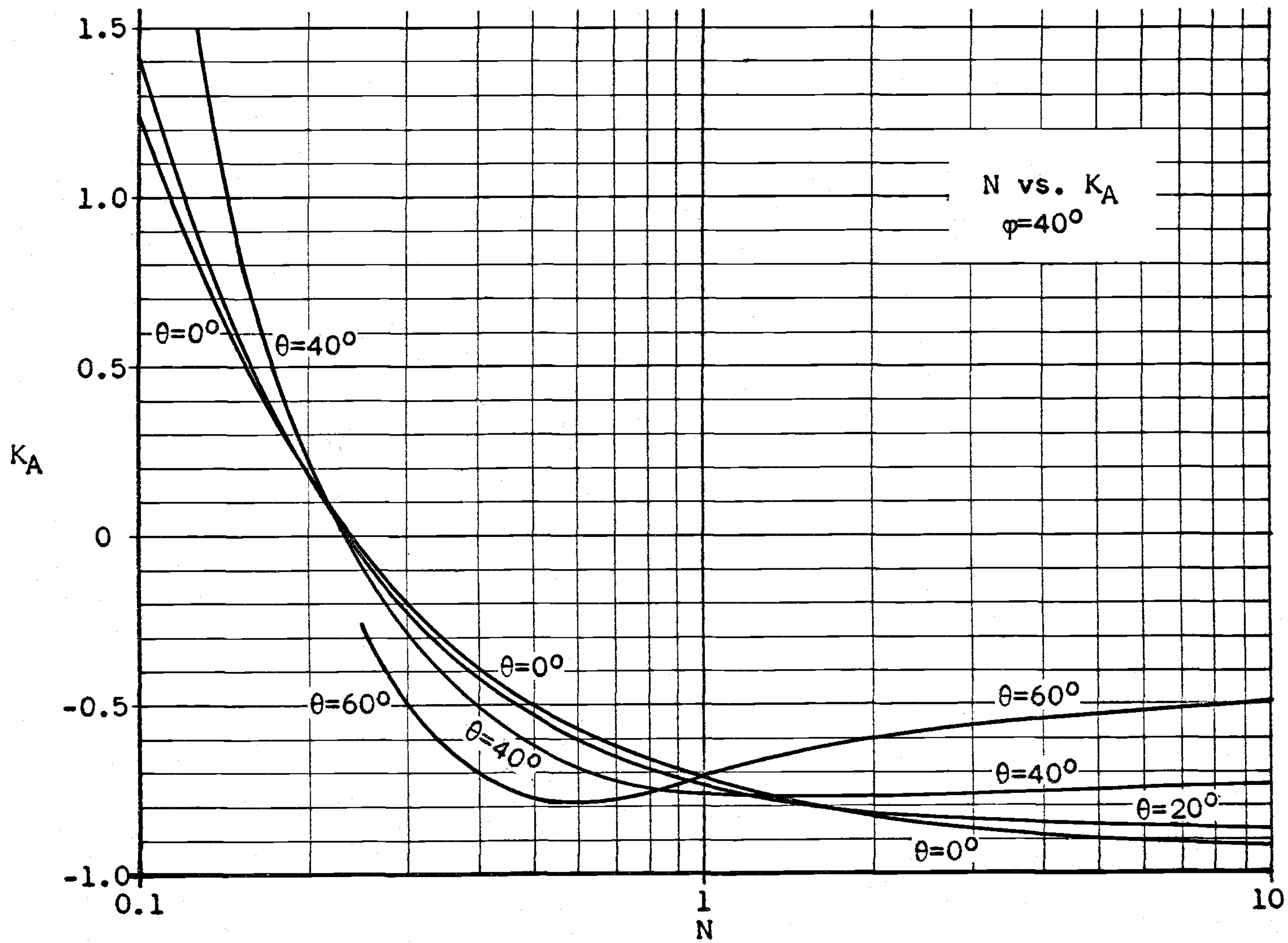
N vs. K_A
$\varphi=40^{\circ}$
K_A
1.5
1.0
0.5
0
-0.5
-1.0
0.1
1
10
N
$\theta=0^{\circ}$
$\theta=40^{\circ}$
$\theta=60^{\circ}$
$\theta=0^{\circ}$
$\theta=40^{\circ}$
$\theta=60^{\circ}$
$\theta=40^{\circ}$
$\theta=20^{\circ}$
$\theta=0^{\circ}$

FIGURE 12

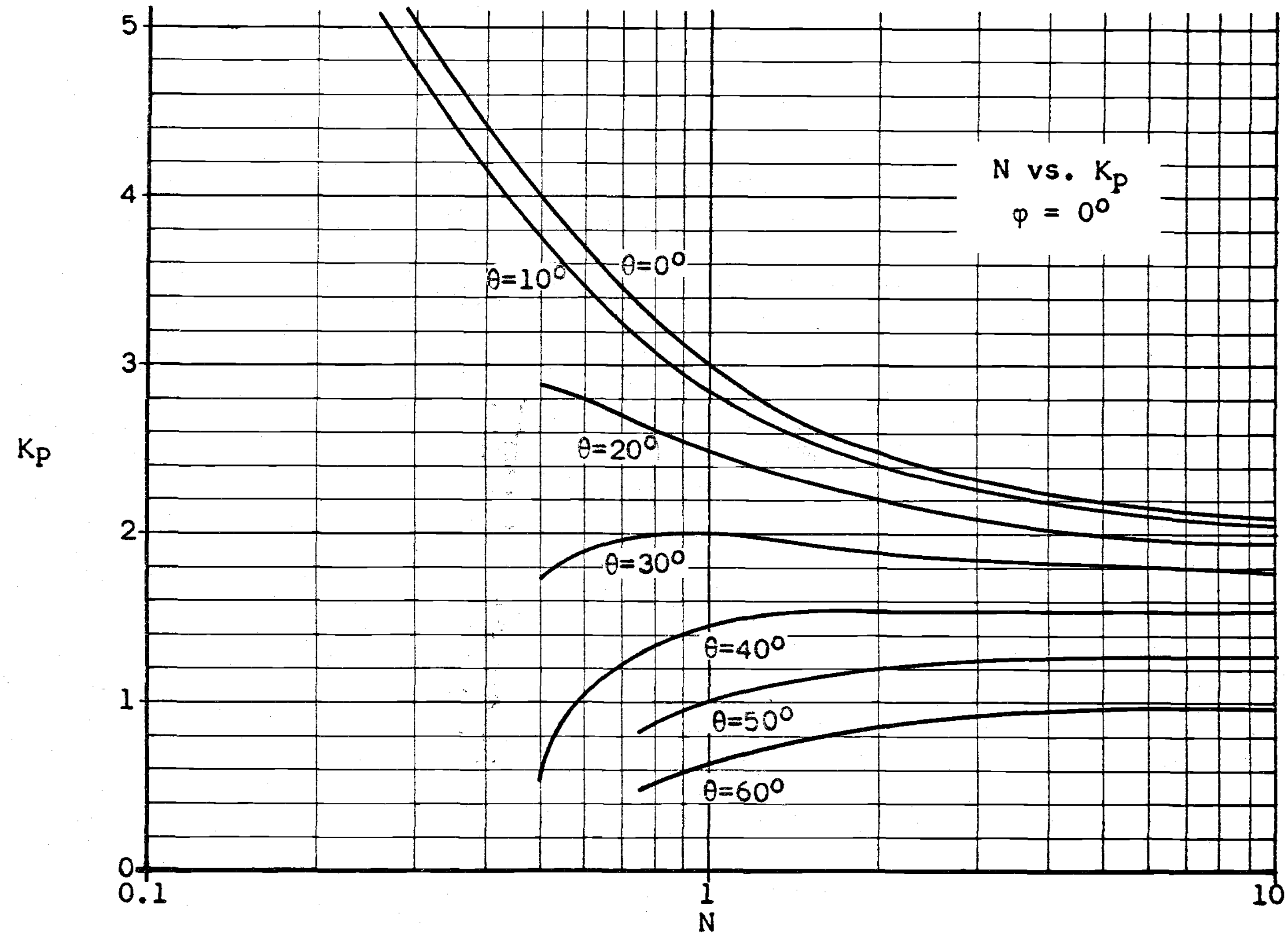

N vs. K_p
$\varphi = 0^o$
K_p
5
4
3
2
1
0
0.1
1
10
N
$\theta=0^o$
$\theta=10^o$
$\theta=20^o$
$\theta=30^o$
$\theta=40^o$
$\theta=50^o$
$\theta=60^o$

FIGURE 13

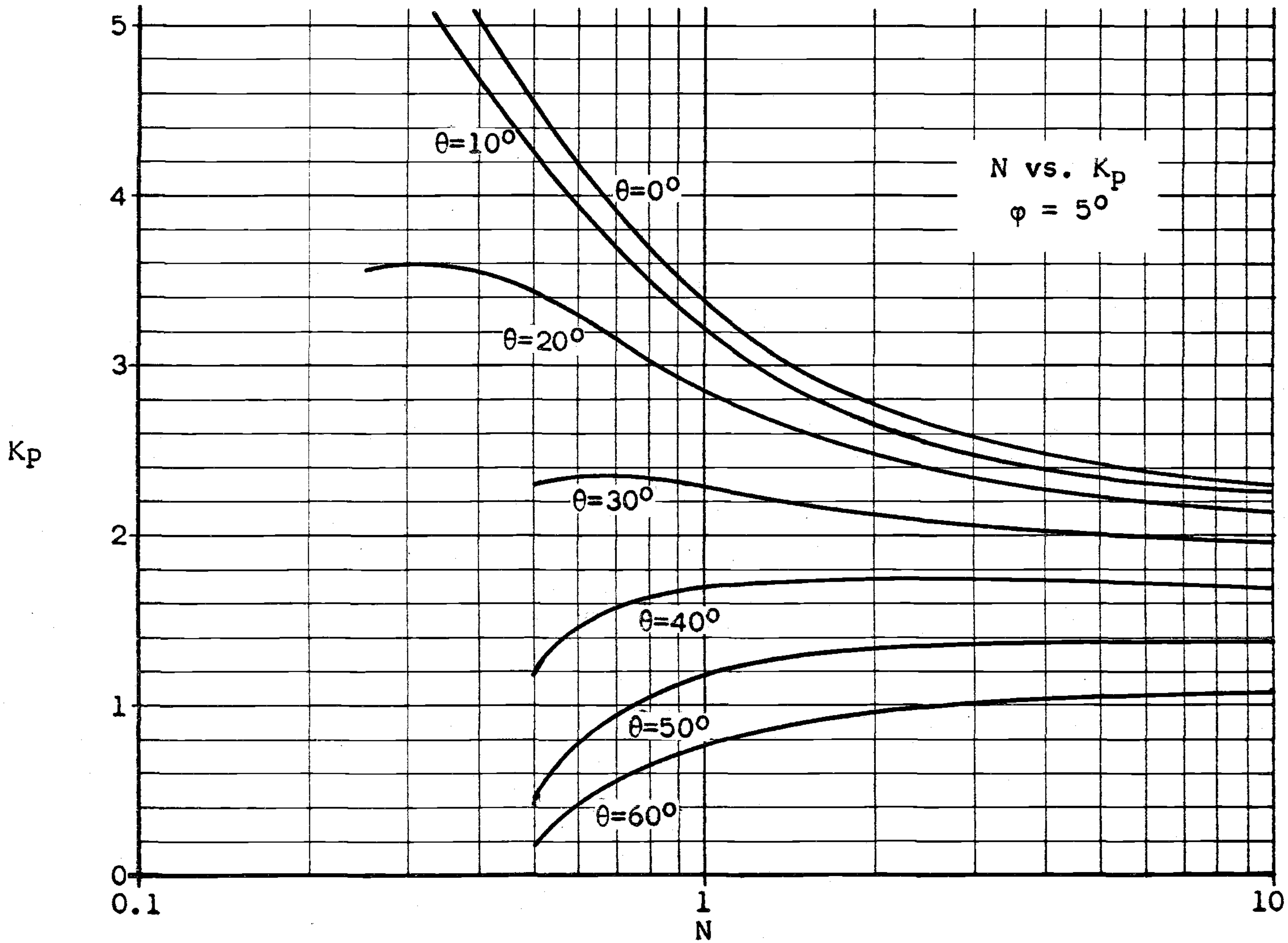
N vs. K_p
$\varphi = 5^o$
$\theta=0^o$
$\theta=10^o$
$\theta=20^o$
$\theta=30^o$
$\theta=40^o$
$\theta=50^o$
$\theta=60^o$
K_p
5
4
3
2
1
0
0.1
1
10
N

FIGURE 14

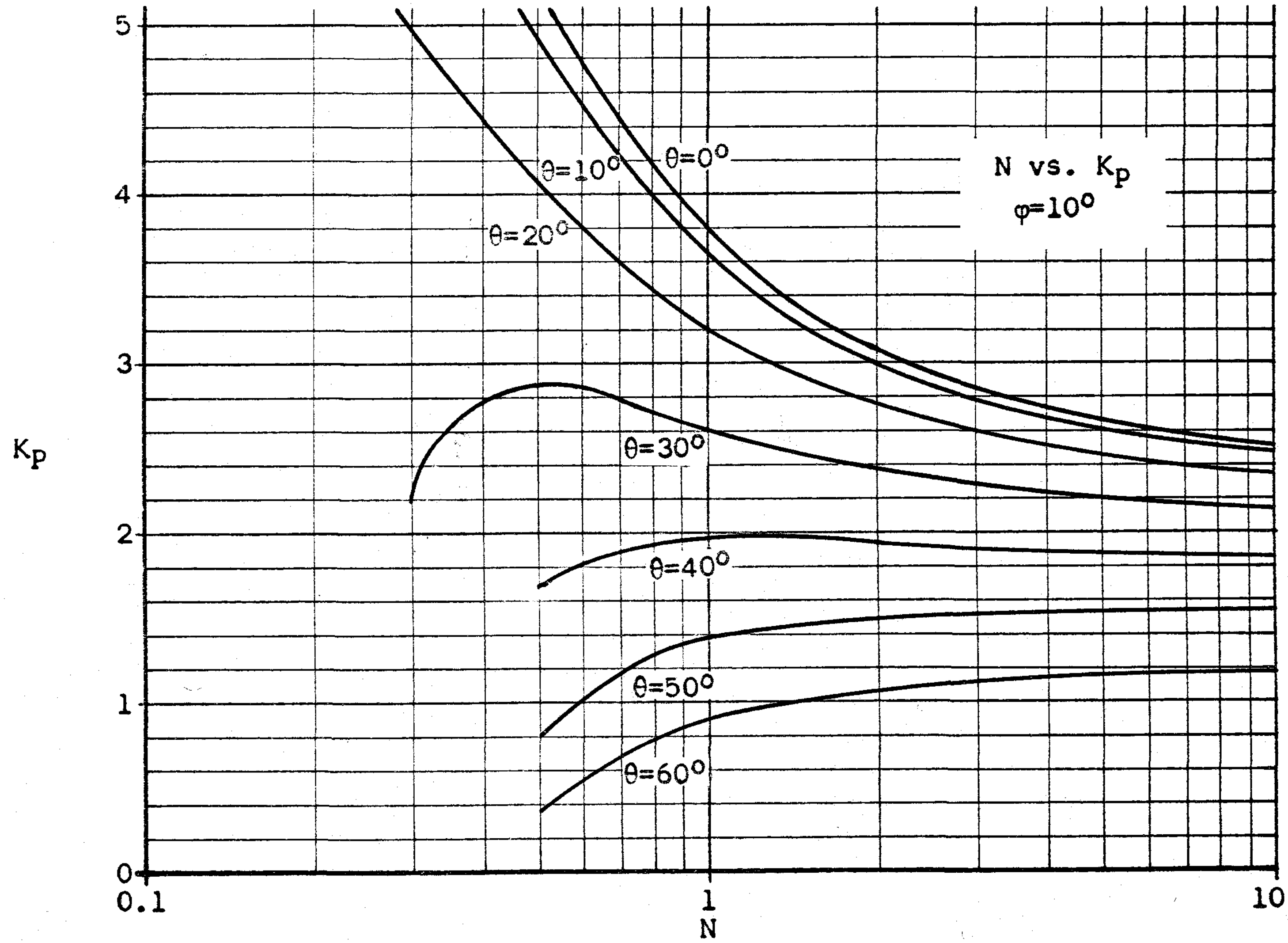
N vs. K_p
$\varphi=10^o$
$\theta=0^o$
$\theta=10^o$
$\theta=20^o$
$\theta=30^o$
$\theta=40^o$
$\theta=50^o$
$\theta=60^o$
K_p
5
4
3
2
1
0
0.1
1
10
N

FIGURE 15

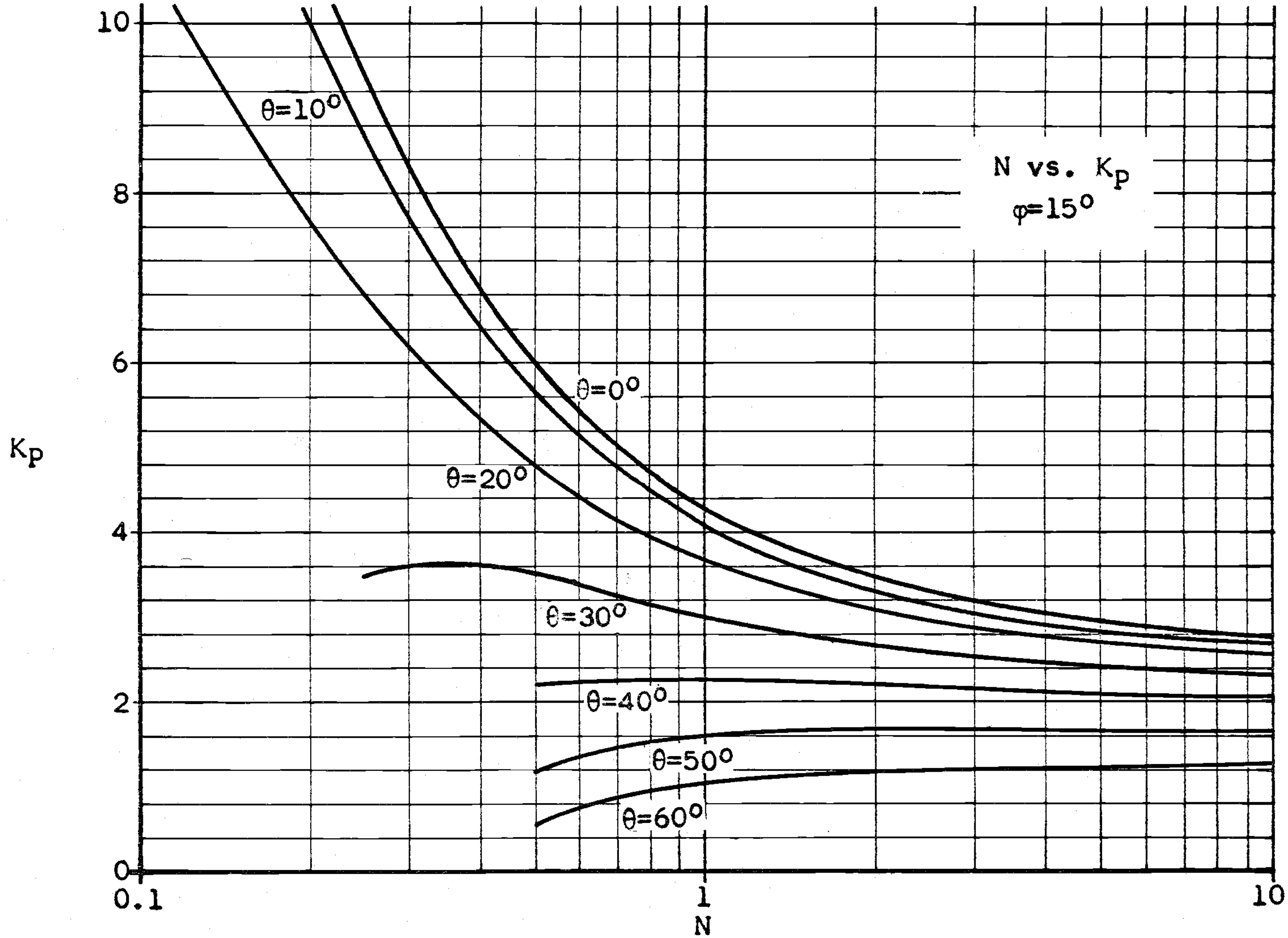
N vs. K_p
$\varphi=15^\circ$
$\theta=0^\circ$
$\theta=10^\circ$
$\theta=20^\circ$
$\theta=30^\circ$
$\theta=40^\circ$
$\theta=50^\circ$
$\theta=60^\circ$
K_p
N
0
2
4
6
8
10
0.1
1
10

FIGURE 16

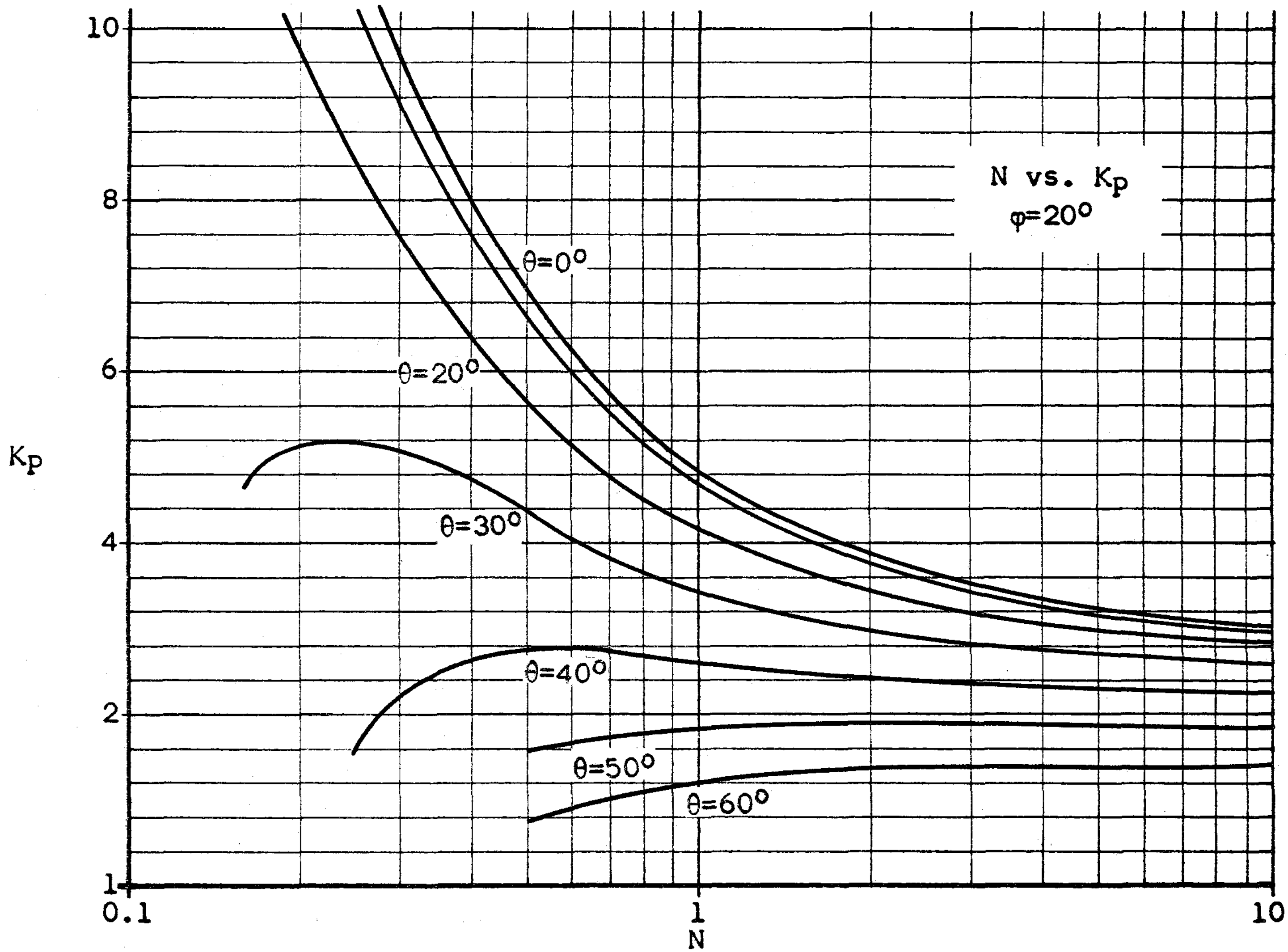

FIGURE 17

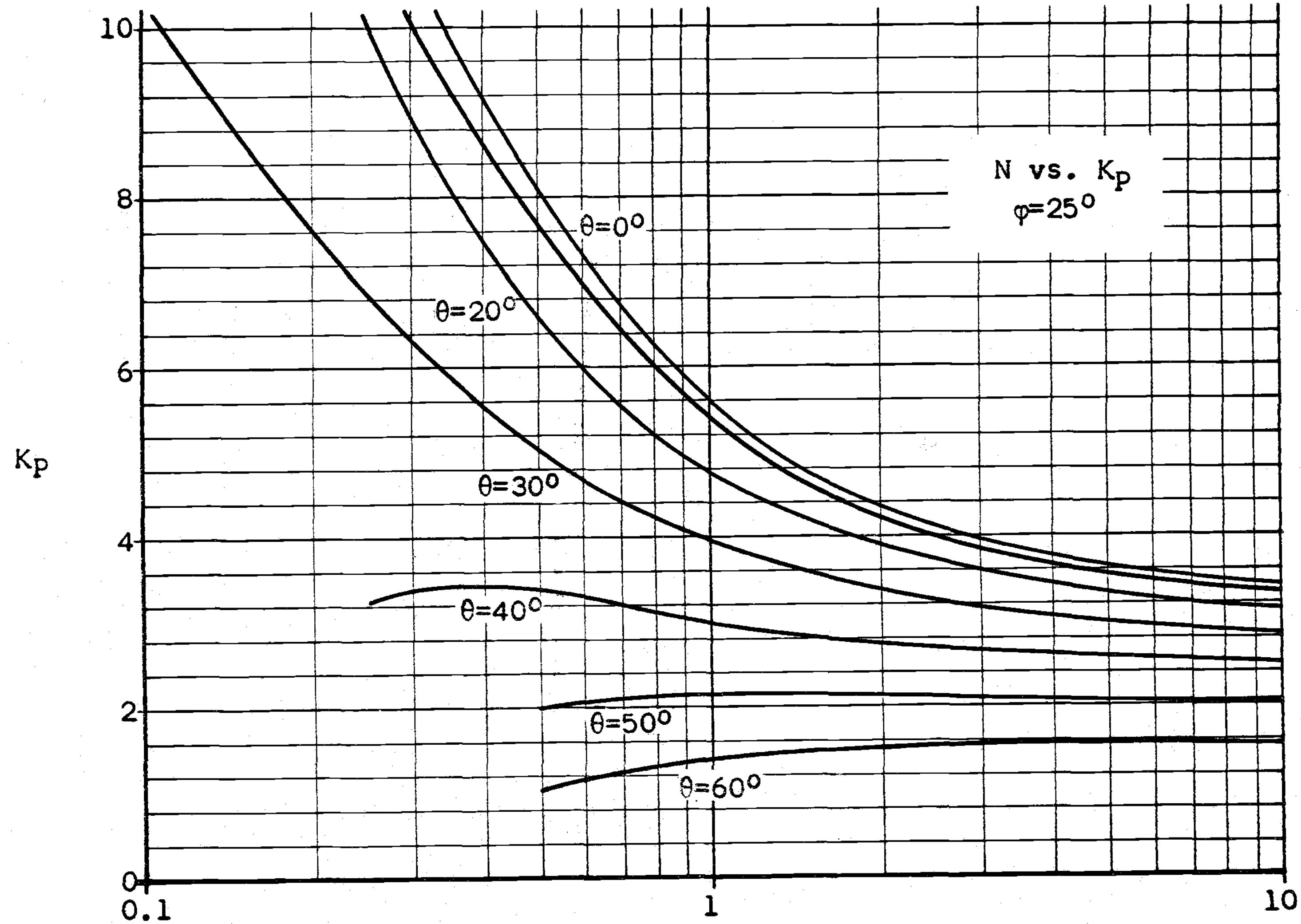
N vs. K_p
$\varphi=25^o$
$\theta=0^o$
$\theta=20^o$
$\theta=30^o$
$\theta=40^o$
$\theta=50^o$
$\theta=60^o$
K_p
10
8
6
4
2
0
0.1
1
10
N

FIGURE 18

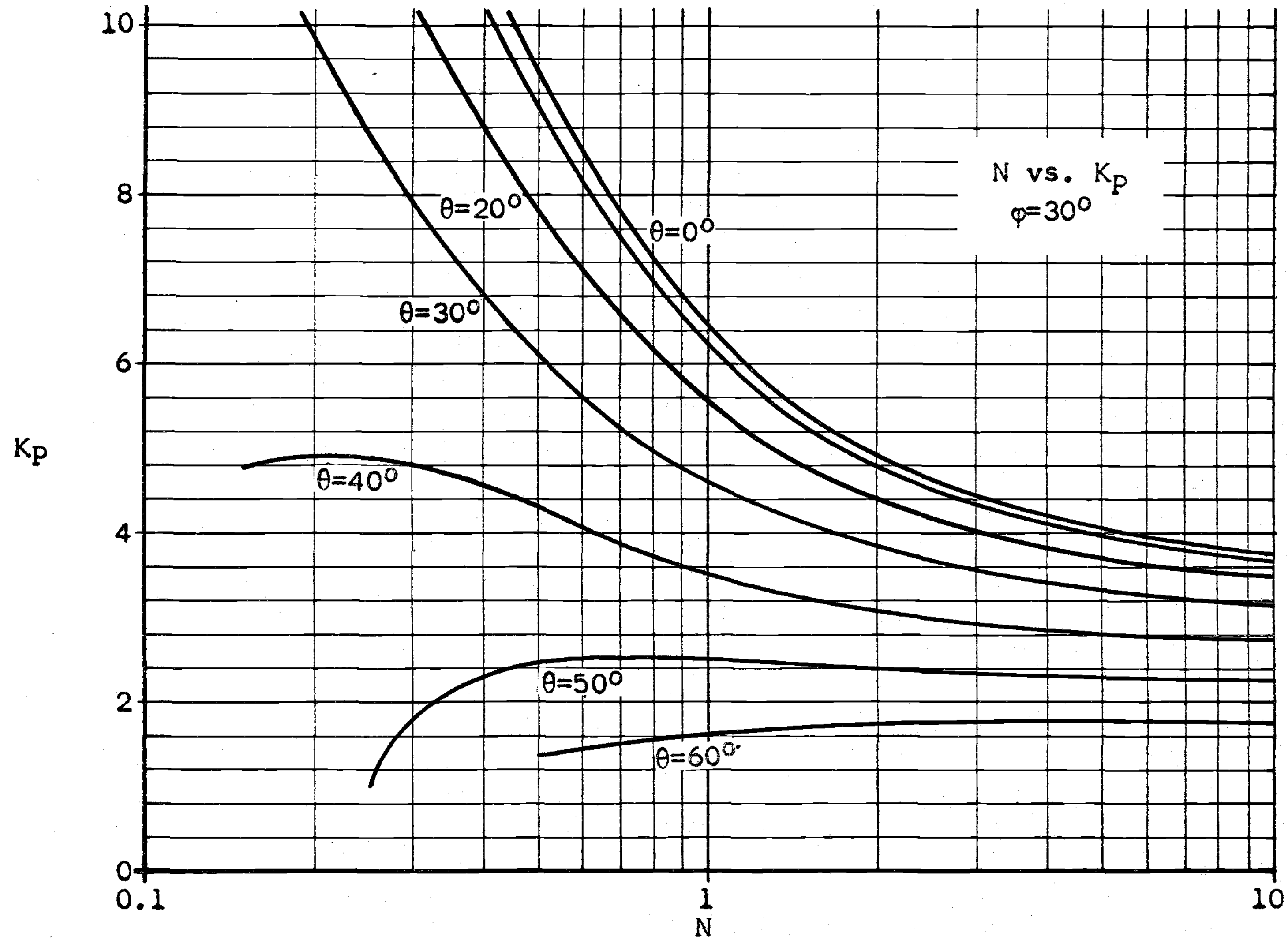

FIGURE 19

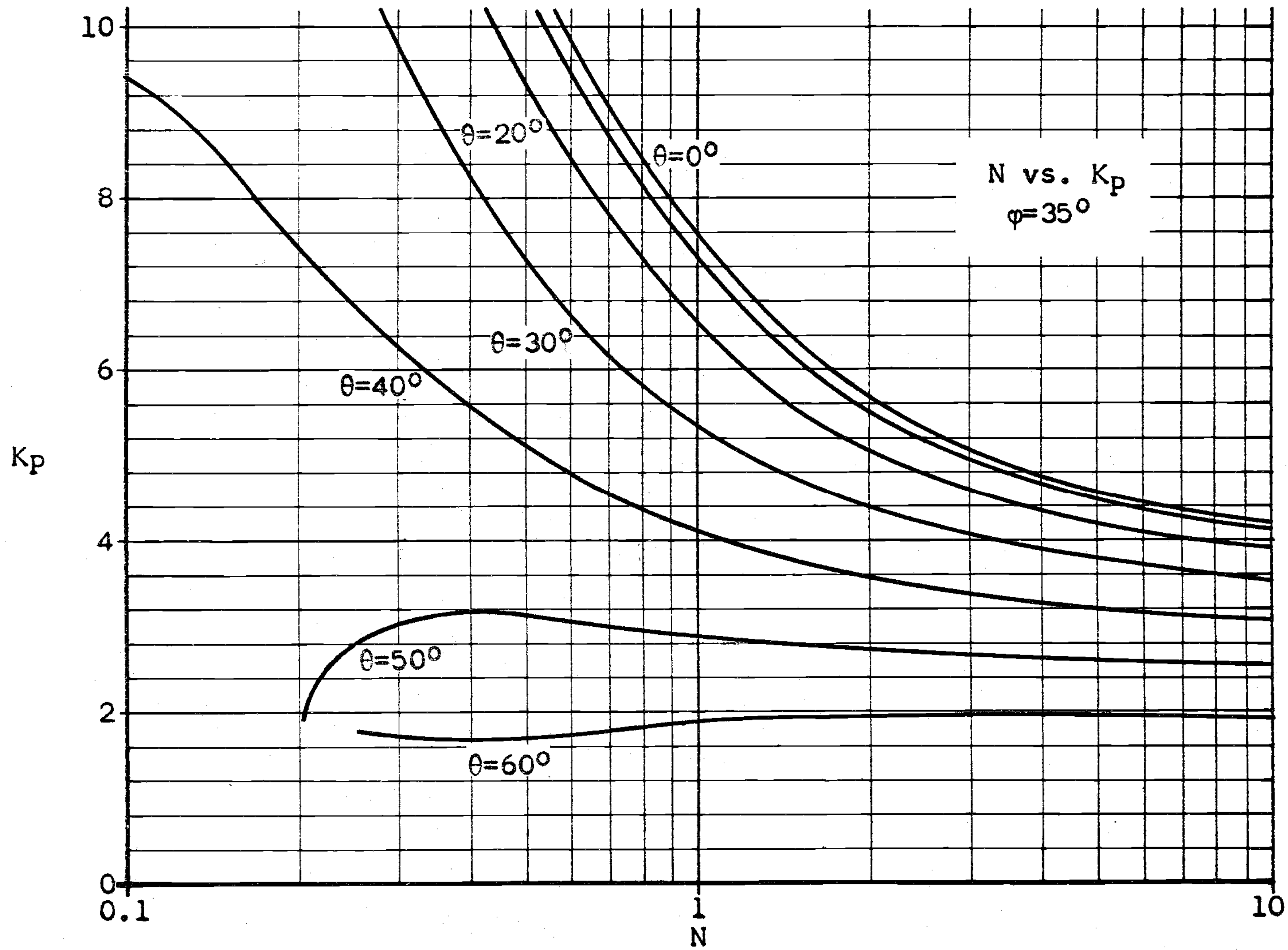

FIGURE 20

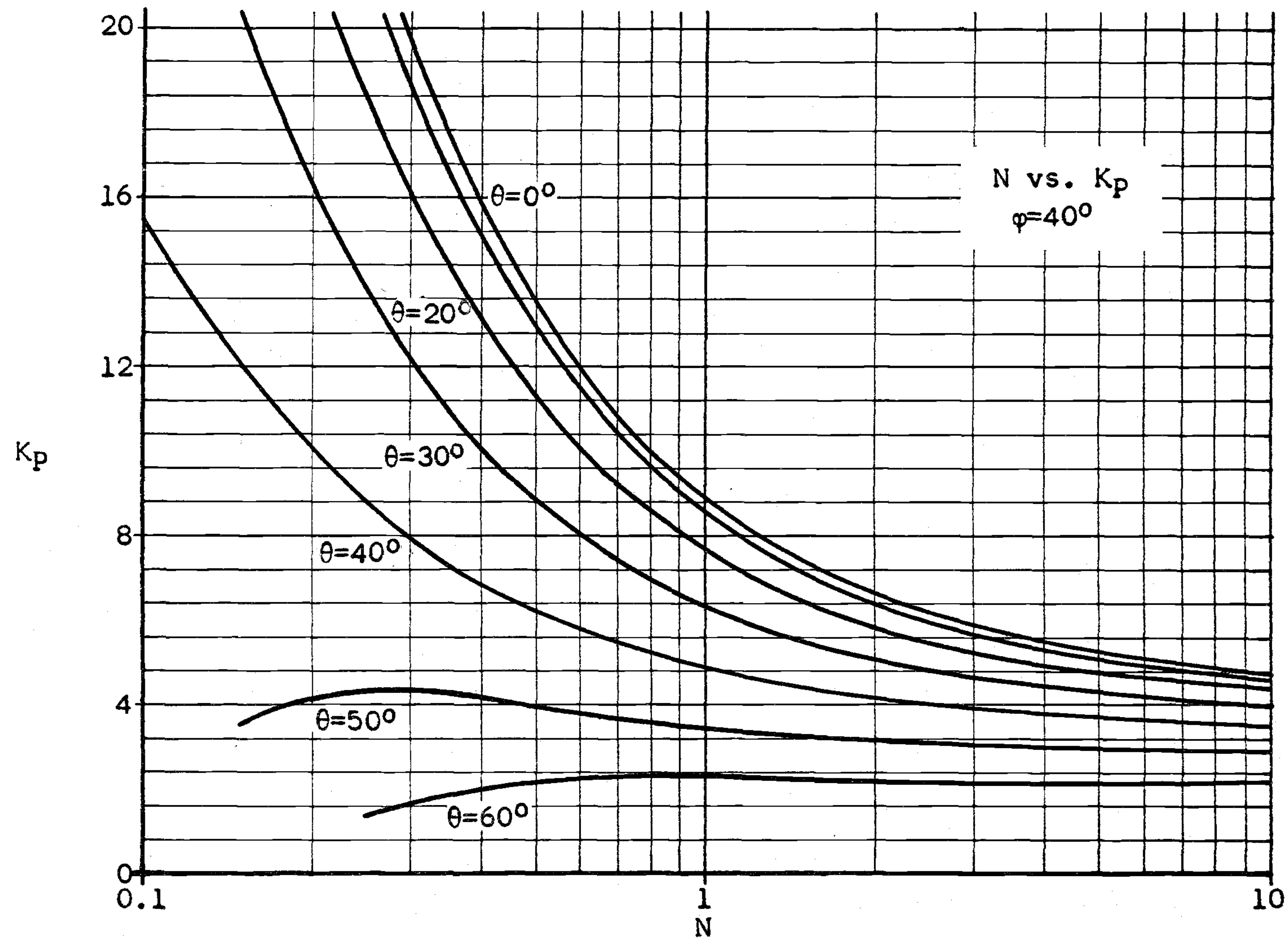

FIGURE 21

DISCUSSION

It has been found in field measurements that the Rankine state of stress is of greater magnitude than the stress developed in actual field conditions when used in retaining wall design in cohesionless materials. In the case of clay soils where soil creep is involved it is doubtful that the developed stresses are as low as the Rankine assumptions indicate. It should not be construed that this paper advocates the use of the Rankine stress condition over those solutions involving more rational assumptions.

It is believed, however, that the simple chart solution would be beneficial in expediting preliminary estimates. It is also conceivable that this solution could be used economically in the design of small retaining walls (i.e. perhaps less than twenty feet in height) where in some cases the cost of a more detailed design procedure would exceed the savings in materials (2, p. 242).

The general solution presented in this paper may be reduced to the following three particular solutions as indicated:

(a) Cohesionless soil, horizontal surface: In Equation (17) let the unit cohesion, c, and the angle of slope, θ, equal zero. The equation then reduces to:

$$\frac{p_A}{\gamma Z} = \frac{\gamma Z}{p_P} = \frac{1-\sin\varphi}{1+\sin\varphi}$$

which agrees with the equation developed by Rankine (3, p. 236).

(b) Cohesionless soil, sloping surface: In Equation (17) let the unit cohesion, c, equal zero. The equation then reduces to:

$$\frac{p_A}{\gamma Z\cos\theta} = \frac{\gamma Z\cos\theta}{p_P} = \frac{\cos\theta-\sqrt{\cos^2\theta-\cos^2\varphi}}{\cos\theta+\sqrt{\cos^2\theta-\cos^2\varphi}}$$

which agrees with Rankine's work (6, p. 424).

(c) Cohesive soil, horizontal surface: In Equation (17) let the angle of slope, θ, equal zero. The equation then reduces to:

$$p_A = \gamma Z\frac{(1-\sin\varphi)}{(1+\sin\varphi)} - 2c\sqrt{\frac{1-\sin\varphi}{1+\sin\varphi}} \quad \text{and}$$

$$p_P = \gamma Z\frac{(1+\sin\varphi)}{(1-\sin\varphi)} + 2c\sqrt{\frac{1+\sin\varphi}{1-\sin\varphi}}$$

which agree with existing equations (7, p. 38)

There are a number of limiting or boundary conditions which also merit discussion, these were used as aids in programming and checking computer operations and are:

(a) When the unit cohesion, c, is zero and the slope angle, θ, exceeds the angle of internal friction, φ, Equation (17) becomes complex since the quantity under the radical sign becomes negative. The physical significance of this is that a cohesionless soil will not stand at a slope exceeding its angle of internal friction.

(b) When the unit cohesion, c, is greater than zero the active stress, p_A, will be zero at some depth, which shall be called the tension depth. Above the tension depth the soil will increase in tensile stress to a maximum at the surface. From the surface to the tension depth the soil will stand vertically unsupported. Below the tension depth the active stress increases in magnitude in a compressive sense. At the tension depth, since the active pressure is zero, G must equal J in Equation (15). Equating these quantities and solving for N:

$$N_{\text{tension depth}} = \cos\varphi/2(1+\sin\varphi)$$

(c) When the unit cohesion, c, is greater than zero and the slope angle, θ, is greater than the angle of internal friction, φ, the tension depth again exists in the slope. In addition to this there is a depth where on Mohr's coordinates the line representing the slope intersects a leaf of the rupture envelope. The depth corresponding to this intersection is known as the critical depth. The critical depth is the maximum depth of the soil on the slope without failure. At depths greater than the critical depth the three conditions placed on Mohr's circle of stresses cannot be satisfied, therefore the equation becomes complex and the quantity under the radical becomes negative. At the critical depth the quantity under the radical is zero and:

$$N_{\text{critical depth}} = (\tan\theta - \tan\varphi)\cos^2\theta$$

If the quantity inside the radical is zero it follows that J in Equations (15) and (16) is zero, and that at the critical depth the active pressure equals the passive pressure. For this case it should be noted also that the passive stress reaches its maximum value at some depth less than the critical depth. This maximum value could be determined by setting the first derivative of Equation (16) equal to zero.

In ensuing extensions of Rankine's work the plane of stress investigation could be considered a variable in addition to the five independant variables treated in this paper.

Another possible area of investigation is to develop an equation which would express the total thrust which is the area of the compressive portion of the pressure diagram. This could be accomplished by integrating Equation (17) between the limits of the tension depth and the desired depth.

Still other possibilities are the incorporation of steady state fluid flow parallel to the surface and the inclusion of a friction value between the soil and the back of a retaining structure.

BIBLIOGRAPHY

1. Capper, P. Leonard and W. Fisher Cassie. The mechanics of engineering soils. 2d ed. New York, McGraw-Hill, 1953. 315 p.

2. Henry, F. D. C. The design and construction of engineering foundations. New York, McGraw-Hill, 1956. 547 p.

3. Hough, B. K. Basic soils engineering. New York, Ronald Press, 1957. 513 p.

4. Rider, Paul R. Analytic geometry. New York, MacMillan, 1947. 383 p.

5. Rouse, Louis J. College algebra. New York, Wiley, 1934. 371 p.

6. Taylor, Donald W. Fundamentals of soil mechanics. New York, Wiley, 1956. 700 p.

7. Terzaghi, Karl. Theoretical soil mechanics. New York, Wiley, 1943. 510 p.